FEBS 28556 FEBS Letters 569 (2004) 307–316

Expression of brain-specific angiogenesis inhibitor 3 (BAI3) in normal brain and implications for BAI3 in ischemia-induced brain angiogenesis and malignant glioma

Hae Jin Kee, Kyu Youn Ahn, Ki Choon Choi, Jung Won Song, Tag Heo, Shin Jung, Jong-Keun Kim, Choon Sang Bae, Kyung Keun Kim*

Research Institute of Medical Sciences and Medical Research Center for Gene Regulation, Chonnam National University Medical School, Kwangju 501-190, Republic of Korea

Received 30 May 2004; accepted 3 June 2004

Available online 15 June 2004

Edited by Jesus Avila

Abstract **Murine brain-specific angiogenesis inhibitor 1 and 2 (mBAI1, mBAI2) are involved in angiogenesis after cerebral ischemia. In this study, mBAI3 was cloned and characterized. Northern and Western blot analyses demonstrated a unique developmental expression pattern in the brain. The level of *mBAI3* in brain peaked 1 day after birth, unlike *mBAI1* and *mBAI2*, which peaked 10 days after birth. In situ hybridization analyses of the brain showed the same localization of BAI3 as BAI1 and BAI2, which includes most neurons of cerebral cortex and hippocampus. In the in vivo focal cerebral ischemia model, *BAI3* expression decreased from 0.5 h after hypoxia until 8 h, but returned to control level after 24 h. The expression of vascular endothelial growth factor following ischemia showed an inverse pattern. The decreased expressions of BAIs in high-grade gliomas were observed, but *BAI3* expression was generally lower in malignant gliomas than in normal brain. Our results indicate that the expression and distribution of BAI3 in normal brain, but not its developmental expression, are very similar to those of BAI1 and BAI2, and that BAI3 may participate in the early phases of ischemia-induced brain angiogenesis and in brain tumor progression.**

Keywords: Brain-specific angiogenesis inhibitor 3; Brain angiogenesis; Cerebral ischemia; Glioma

1. Introduction

Recently, human BAI1 (hBAI1), a novel brain-specific gene, was isolated by the strategy of identifying genomic DNA fragments containing functional p53 binding sites [1]. The murine phytanoyl-CoA alpha-hydroxylase-associated protein 1, a protein related to the Refsum disease gene product, was found to interact with the cytoplasmic region of hBAI1 through yeast two-hybrid screening, and we cloned the murine BAI1 homologue (mBAI1) [2]. The seven-span transmembrane region (STR) and two functional elements, an Arg-Gly-Asp (RGD) motif and thrombospondin type 1 repeats (TSRs) are well conserved between hBAI1 and mBAI1. The TSR can inhibit experimental angiogenesis induced by basic fibroblast growth factor in the rat cornea [3], and also is present in several proteins involved in the guidance of nerve growth cones and axonal growth, such as UNC-5 and F-spondin [4].

Two novel human genes homologous to hBAI1 have been identified and designated as hBAI2 and hBAI3. Analysis of their predicted proteins shows that the TSR and STR are well conserved among the three BAIs. Like hBAI1, the other two genes are specifically expressed in brain and it appears likely that the three hBAIs are closely related. However, the extracellular and cytoplasmic domains are relatively different among them [5]. In a study using the rat focal cerebral ischemia injury model produced by the occlusion of the middle cerebral artery, we showed that the expression of *BAI1* decreased on the ischemic side [2]. Also, we showed that BAI2 is involved in ischemia-induced brain angiogenesis [6]. To date, the functions of neuron-specific BAI3 in the brain are unknown.

Glioblastoma is a highly vascularized and high-grade solid tumor of the central nervous system. Angiogenesis is a prominent feature of glioblastoma but the mechanisms involved in the control of this process are not completely understood [7]. The angiogenic factors that have been implicated in glioma angiogenesis are vascular endothelial growth factor (VEGF) and basic fibroblast growth factor. Hypoxia-inducible factor 1α (HIF-1α) initiates the transcription of a number of hypoxia-inducible genes including VEGF [8]. Recently, it was reported that the expression of BAI1 is absent in most glioma cell lines and in most human glioblastomas [9]. However, the expression of the other two BAI genes and their relevance in the progression of glioma were not reported.

In this study, we cloned mouse BAI3 and investigated its expression and distribution in the brain. We examined the angiostatic characteristics of BAI3 in the rat focal cerebral ischemia injury model, and also examined whether the expression of the three BAIs and certain angiogenic factors were changed in different grades of human glioma. We found that

* Corresponding author. Fax: +82-62-232-6974.
E-mail address: kimkk@chonnam.ac.kr (K.K. Kim).

Abbreviations: mBAI1, mBAI2, and mBAI3, murine brain-specific angiogenesis inhibitor 1, 2 and 3; VEGF, vascular endothelial growth factor; hBAI1, human BAI1; STR, seven-span transmembrane region; TSR, thrombospondin type 1 repeat; HIF-1α, Hypoxia-inducible factor 1α; PBS, phosphate buffered saline; aa, amino acids; TSP, thrombospondin; EC, endothelial cells; GPS, G protein-coupled receptor proteolysis site; GPCR, G-protein coupled receptor

0014-5793/$22.00
doi:10.1016/j.febslet.2004.06.011

neuron-specific BAI3, like BAI1 and BAI2, probaby participates in the regulation of ischemia-induced brain angiogenesis and in the progression of glioma.

2. Materials and methods

The investigation conforms to the *Guide for the Care and Use of Laboratory Animals* published by the US National Institutes of Health (NIH Publication No. 85-23, revised 1996). The Ethics Committee of Chonnam National University Medical School approved all experimental protocols, including the use of surgically resected specimens.

2.1. Tumor samples

All tumor specimens were obtained from patients undergoing therapeutic operation for brain tumors at Chonnam University Hospital (Kwangju, Korea) from 2000 to 2003. All glioma samples were classified according to the World Health Organization classification of brain tumors (low-grade, grade III, and grade IV). The low-grade glioma used consisted of 1 pilocytic astrocytoma (patient #1), 1 astrocytoma (patient #2), 1 astrocytoma of grade II (patient #3), 2 ependymomas (patients #4 and #5), and 1 oligodendroglioma of grade II (patient #6). Grade III tumors consisted of 2 anaplastic mixed gliomas (patients #7 and #8), 2 anaplastic ependymomas (patients #9 and #10), 2 anaplastic oligodendrogliomas (patients #11 and #12). Grade IV tumors consisted of 4 glioblastomas (patients #13–16). Normal brain tissue was obtained from 1 patient with head trauma from a traffic accident.

2.2. Isolation of murine BAI3 cDNA

A murine cDNA spanning nucleotides 3868 through 4391 was generated by RT-PCR using oligonucleotides based on the human sequence [5]. Total RNA from mouse brain (400 ng) was used as the template. The human sense and antisense primers were 5′-AGAGGGGCTGACATGGACATAG-3′ and 5′-GCAGGGTTTTCCATACTGCTTG-3′, respectively. The resulting 524-bp product was subcloned into the TA vector cloning system (Invitrogen), and the identity of the cDNA was confirmed by sequencing. The GenBank BLAST homology-search program was used to search for this sequence. The cDNA insert corresponded to the cytoplasmic region of mBAI3. This cDNA fragment was then used to screen the mouse brain lambda ZAP II cDNA library to obtain the full-length cDNA of mBAI3 (Fig. 1). The mBAI3 cDNA has been deposited in the GenBank database (NM 175642).

2.3. Northern blot and RT-PCR analyses

Total RNAs were extracted from the mouse (BALB/c) tissues, and normal or ischemic mouse brain tissues, and tumor tissue of each glioma patient as described [10]. For Northern analysis, total RNA (10 μg) was denatured with glyoxal, separated by size on 1.0% agarose gels, and transferred to Genescreen (Dupont). Probes (mBAI3, nucleotide residues 3661–4056) were radiolabeled by nick translation, and hybridization and signal visualizations were performed as described [10]. In all experiments, the integrity of the RNA samples was established by Northern analysis with a mouse β-actin or GAPDH probe. The intensity of the bands was quantified by imaging densitometry with the Gel Documentary System (DOC 2000 model, Bio-Rad), and each transcript level of BAI was normalized with respect to the corresponding GAPDH level.

Reverse transcription was performed at 42 °C for 60 min (200 ng of total RNA, 100 pmol random primers, reverse transcriptase). The RT-PCR exponential phase was determined to be 30 cycles to allow quantitative comparisons among the cDNAs from identical reactions. Cycling conditions were: initial denaturation at 94 °C for 5 min followed by 30 cycles at 94 °C for 1 min, appropriate annealing temperature for 1 min, and 72 °C for 2 min (Mastercylcer Personal PCR system, Eppendorf). The annealing temperature was 60 °C for mBAI3 and β-actin. The amplification products were analyzed on agarose gels and visualized by UV epifluorescence following ethidium bromide staining. Also, RT-PCR was performed with primers for β-actin as a control. PCR primers were as follows: sense, 5′-GAATTTGGAATGATGGGAGATC-3′ and antisense, 5′-GATAATCCTCTGGGCATATTTC-3′ for TSR of mBAI3; sense, 5′-CTCTAT-GCCTTCGTTGGACCTG-3′ and antisense, 5′-CATGGCCAGAACTGCAGACATC-3′ for third loop of STR in mBAI3; sense, 5′-GATGATATCGCCGCGCTCGTC-3′ and antisense, 5′-AGCCAGGTCCAGACGCAGGAT-3′ for mouse β-actin.

To investigate the expression level of anti-angiogenic factors (BAI1, BAI2, BAI3, TSP1), angiogenic factors (VEGF, HIF-1α), and the p53 gene in human glioblastoma, we also employed an RT-PCR assay. PCR primers were as follows: sense, 5′-ATGACCGACTTCGAGAAGGACG-3′ and antisense, 5′-TCTGCGGCATCTGGTCAATGTG-3′ for hBAI1; sense, 5′-GTGTCCAGCCTTCCATGAGATG-3′ and antisense, 5′-TTTCCGCATCCACCATGAAGC-3′ for hBAI2; sense, 5′-GAATTTGGAATGATGGGAGATC-3′ and antisense, 5′-GATAATCCTCAGGGCATATTTC-3′ for hBAI3; sense, 5′-CGTCCTGTTCCTGATGCATG-3′ and antisense, 5′-GGCC-CTGTCTTCCTGCACAA-3′ for hTSPl; sense, 5′-TGCCATCCAATCGAGACCCTG-3′ and antisense, 5′-ATCTGGTTCCCGA-AACGCTGAG-3′ for hVEGF; sense, 5′-AAGCCCTGAAAGCGCAAGTCC-3′ and antisense, 5′-TG-CATGATCGTCTGGCTGCTG-3′ for hHIF-1α; sense, 5′-AAGCAATGGATGATTT-3′ and antisense, 5′-AGCTGTTCCGTCCCAGTAGA-3′ for p53. RNA integrity was confirmed with parallel RT-PCR amplification using β-actin primers.

2.4. Production of the anti-mBAI3 antibody and Western blot analysis

A GST-mBAI3 fusion construct was prepared by amplifying the nucleotide residues 3661–4056 (a region unique to mBAI3) of murine BAI3. The fragment was cloned into the unique *Bam*HI and *Eco*RI sites of pGEX-2T and purified as previously described [2]. Rabbit polyclonal antiserum recognizing mBAI3 was prepared using the GST-mBAI3 fusion protein. The serum recognizing mBAI3 was passed through a column of GST-mBAI3 fusion protein, and the column was eluted with a low-pH buffer to obtain the anti-GST-mBAI3 antibody. The eluate was further purified by passage through a column of GST protein to remove the anti-GST antibody component. Cell lysates were prepared from mouse tissues using a lysis buffer containing 1% Triton X-100, and resolved by SDS–PAGE. Resolved proteins were transferred to a nitrocellulose membrane and blotted with anti-BAI3 serum and anti-rabbit Ig-HRP (Ammersham) as previously described [10]. The intensity of the bands was quantified by imaging densitometry with the Gel Documentary System (DOC 2000 model), and each protein level of BAI3 or VEGF was normalized with respect to the corresponding actin level.

2.5. In situ hybridization

Sprague–Dawley rats (200–230 g) were anesthetized with an intraperitoneal injection of sodium pentobarbital (50 mg/kg), and the brain was fixed by in vivo perfusion of the abdominal aorta with 4% paraformaldehyde in a phosphate buffered saline (PBS) for 10 min. The brain was excised and then immersed in the same fixative for 3 h at 4 °C. The tissue blocks were washed in PBS, dehydrated in a graded series of ethanol washes, and embedded in paraffine. Tissue sections were cut at 6 μm and mounted on gelatine-coated glass slides. Sense and anti-sense probes specific for the mBAI3 were generated from the recombinant plasmid (nucleotides 3661–4056), using T3 and T7 RNA polymerases in the presence of digoxigenin-11-UTP (Boehringer Mannheim). In situ hybridization was performed as described previously [2]. Briefly, the tissue sections were deproteinated and acetylated. Prehybridization was conducted at 48 °C for 4 h in a humidified chamber. The slides were then hybridized with 20 ng/μl digoxigenin-11-UTP-labeled riboprobe in a hybridization buffer at 48 °C for 14–16 h. Hybridizations with the sense probes were performed in parallel with the anti-sense probes on adjacent sections. Unbound probe was removed by sequential washes of SSC with or without 20 μg/ml ribonuclease. RNA–RNA hybrids were immunodetected with a 1:500 dilution of anti-digoxigenin alkaline phosphatase conjugate, followed by incubation with nitro blue tetrazoliurn salt and 5-bromo-4-chloro-3-indolyl phosphate. After mounting in a crystal mount medium, the sections were photographed on a light photomicroscope.

2.6. Focal ischemia model in rat

Sprague–Dawley rats (200–230 g) were anesthetized with 4% halothane in an anesthetic chamber and maintained with 1% halothane in 100% O_2 using a rodent mask. Operation for focal ischemia was performed as described previously [6]. Briefly, the right common carotid artery (CCA) was exposed and then the external carotid artery (ECA) was transected 2 mm distal from the carotid bifurcation after being ligated by 4-0 silk suture. The internal carotid artery (ICA) was then

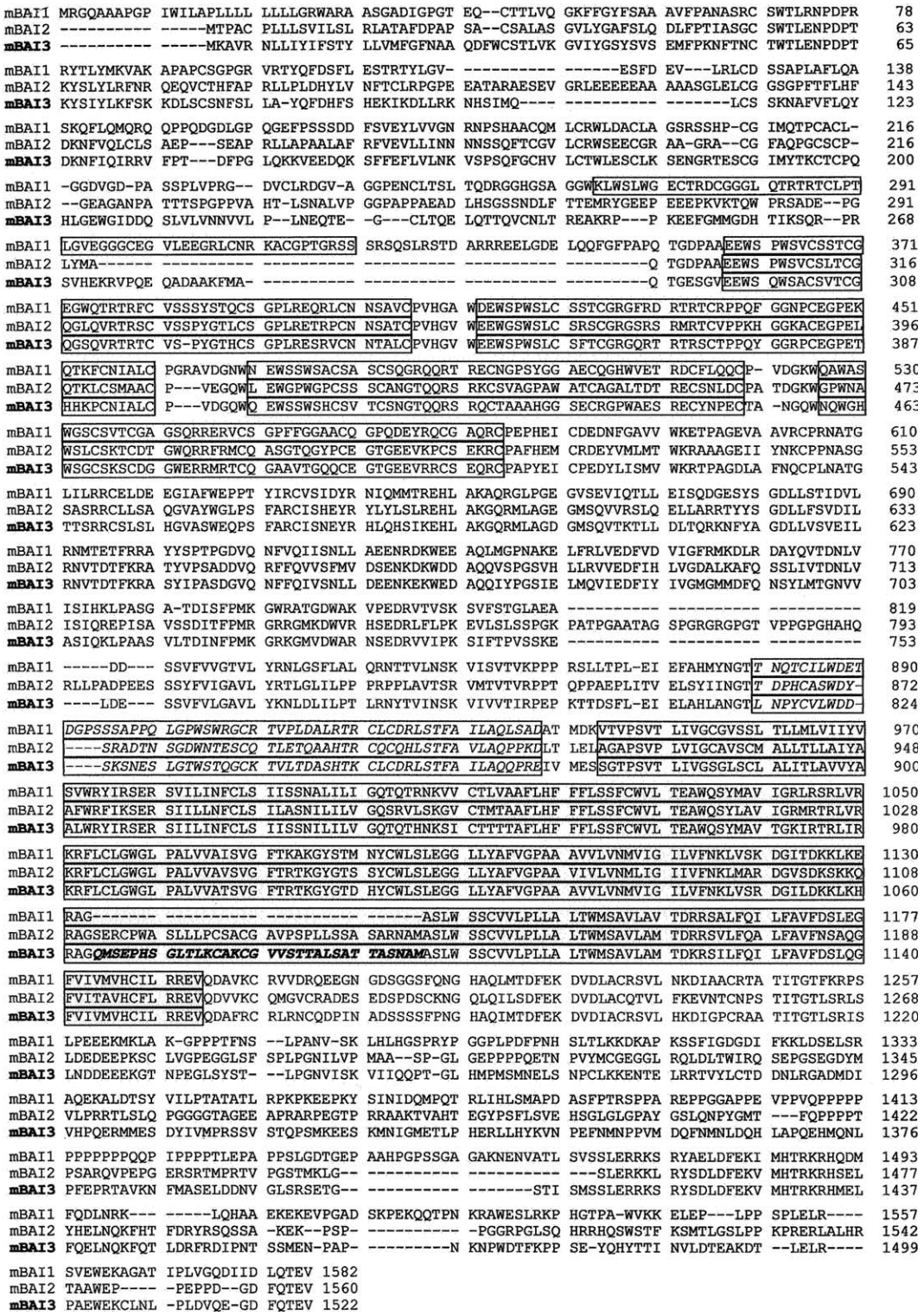

Fig. 1. Deduced amino acid (aa) sequence of mBAI3 compared with mBAI1 and mBAI2. The mBAI2 and mBAI3 sequences are shown below the mBAI1 sequence. The gaps introduced for maximal alignment are marked with dashes. mBAI3 is a 1522-aa protein (4569-bp transcript) with a deduced molecular mass of 171-kDa. Thrombospondin type I repeats (TSR) and seven-span transmembrane regions (STR) are indicated in open and filled box, respectively. The aa in the TSR and STR are well conserved among them. GPS (G protein-coupled receptor proteolysis site) domain is represented by italic characters in the open box just before the STR region. The third cytoplasmic loop of STR, which is deleted in the splice variant of mBAI3 (mBAI1-ΔSTR) is represented by bold italic characters in the filled box.

isolated. The CCA and ICA were occluded with microvascular clips. A 3-cm length of 4-0 monofilament suture with a slightly enlarged tip was introduced into a hole in the ICA, and then the microvascular clip in the ICA was removed. The suture was then gently advanced about 18 mm into the ICA and circle of Willis to cross the opening of the middle cerebral artery. The rat was sacrificed after the time course of ischemia

(0.5, 2, 4, 8, 24 h), and the brain was exposed. Brain slices were stained with 2% triphenyl tetrazolium chloride to visualize and measure the infarct volumes in each group [2]. The ischemic portion of the cerebral cortex and the contralateral portion of the normal cerebral cortex were removed for protein preparation.

3. Results and discussion

3.1. Cloning of the murine BAI3 cDNA

A set of oligonucleotide primers capable of amplifying the unique cytoplasmic region of the human *BAI3* transcript was used to amplify the corresponding region of the murine BAI3 mRNA. The resulting 524-bp amplification product was subcloned and sequenced to confirm its identity (nucleotides 3868–4391 of mBAI3). This fragment was then used to screen a mouse brain lambda ZAP II cDNA library and several positive clones were obtained. Database searches with the deduced amino acid sequence identified a high degree of identity (92.5%) between one of positive clones (#104) and hBAI3. This murine cDNA fragment was then used to rescreen the mouse brain cDNA library, and several clones (#101, #107, #109) were isolated (data not shown). Clone 107 had start codon, and clone 109 had a stop codon. The overlapping clones spanned a total of 4597 bp.

Sequence analysis of the cDNA identified an open reading frame that could direct the synthesis of a protein of 1522 amino acids (aa), with a calculated molecular mass of 171 kDa. The termination codon of the open reading frame was located at nucleotides 4567–4569. Database surveys identified a high degree of deduced amino acid sequence identity (98.4%) between this cloned gene product and hBAI3 over the full length of the molecule. Based on this high degree of homology, we identified our cloned gene product as murine BAI3. The deduced amino acid sequences of the mBAI3, mBAI2 and mBAI1 genes are shown in Fig. 1. The TSR in the extended extracellular domain and the STR are located at the same positions and highly conserved among them. However, the cytoplasmic region (1262–1371 aa) of mBAI3 was divergent from that of mBAI2 (1311–1416 aa) and mBAI1 (1299–1371 aa) genes (Fig. 1). This divergence indicates that BAI-interacting proteins that bind to this cytoplasmic region might differ among the three proteins. The presence of alternative splicing in the third cytoplasmic loop of the STR was confirmed by RT-PCR (Fig. 4G).

The predicted structure of the mBAI3 protein includes extended extracellular and cytoplasmic domains, a GPS (G protein-coupled receptor proteolysis site) domain, and an STR (Fig. 2A). The STR (748–1176 aa) and Latrophilin/CL-1-like GPS domain were present in mBAI3, as in mBAI1 and mBAI2. Thus, mBAI3 was assumed to be a G-protein coupled receptors (GPCRs) in the brain having a GPS domain and STR. mBAI3 has 4 TSRs, as does mBAI2, while mBAI1 has 5 TSRs, though the functional significance of this difference is unknown. The conserved domains observed in mBAI3 give some indication of its possible function. Thrombospondin-1 (TSP1) and thrombospondin-2 (TSP2), two TSR-containing proteins of the TSP family, possess antiangiogenic activity [11,12]. In contrast, thrombospondin-3, which lacks TSRs, has no inhibitory activity on human dermal microvascular endothelial cell (EC) proliferation, confirming that TSRs elicit the antiangiogenic activity of TSP1 and TSP2 [13]. The TSR contains two subdomains that may independently influence the

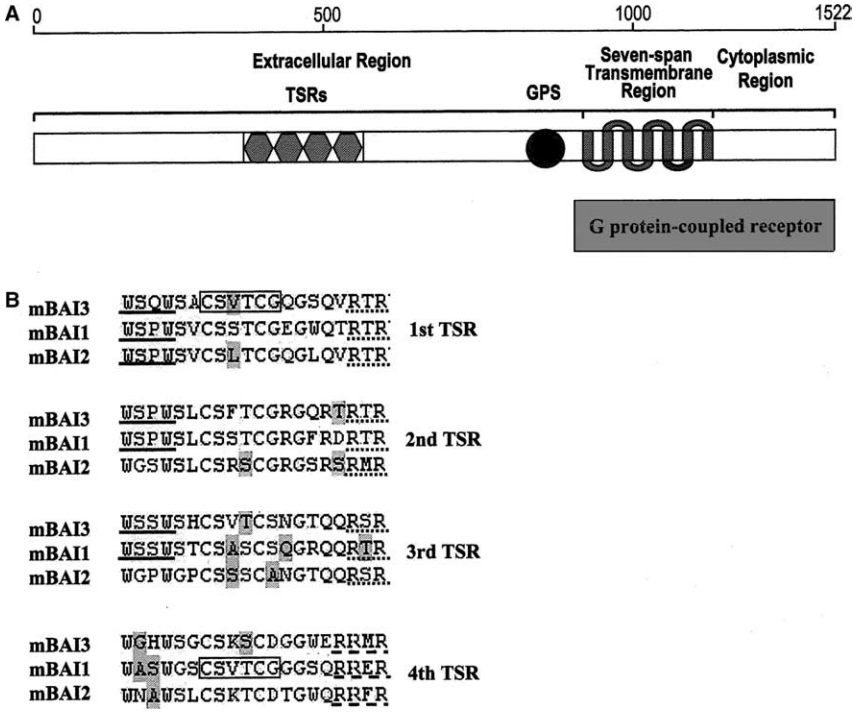

Fig. 2. Schematic representation of the conserved domain in mBAI3 protein and comparison of cell-binding motifs among BAIs. (A) mBAI3 has 4 TSRs, a GPS domain in the extracellular region, and an STR, suggesting that BAI3 may be a G-protein-coupled receptor in the brain. (B) The cell/glycoconjugate-binding motif together with flanking sequences from 4 TSRs of mBAI3 is aligned with the corresponding sequences of mBAI1 and mBAl2. WSXW is underlined, CSVTCG is boxed, CSXTCXXXXXXRXR is drawn with a dotted line, and BBXB is represented with a broken line.

process of neovascularization, and synthetic peptides derived from the TSR have been found to have potent antiangiogenic activity in vivo and in assays of EC function [3,14].

The WSXW and CSXTCXXXXXXRXR motifs were found in 3 TSRs, but not the fourth TSR, in all 3 mBAIs (Fig. 2B). Actually, mBAI1 has another TSR before 1st TSR, but it is not shown in Fig. 2B. The CSVTCG motif was identified in the first TSR of mBAI3 (Fig. 2B). It has been reported that the WSXW, CSXTCXXXXXXRXR, and CSVTCG motifs are involved in cell binding [4]. In the fourth TSR of the three mBAIs, a BBXB motif (B representing a basic aa residue) is present instead of a WSXW motif (Fig. 2B). BBXB, located adjacent to the WSXW motif, is also a cell-binding motif. Previous studies showed that the peptide sequence CSVTCG within the TSR of TSP1 interacts with a surface receptor glycoprotein, CD36 [15]. The CSVTCG peptide mediates the in vitro and in vivo inhibitory effects of TSP1 on ECs [12,16]. The first TSR of BAI3 may be important to antiangiogenic activity because it contains a CSVTCG motif for CD36 binding. mBAI3 also has CSFTCG (2nd TSR) and CSVTCS (3rd TSR) sequences, similar to the CSVTCG motif. Properdin, which has 6 TSRs, plays an important role in full complement activity [17]. However, properdin lacking the fourth TSR, which contains the sequence CPVTCG, is unable to stabilize the alternative pathway C3 convertase [18]. Using the NCBI conserved domain search, we also found that the 4 TSR domains of mBAI3 align well with spondins, serine proteinase inhibitor with TSRs, and disintegrin metalloproteinases with TSRs.

The GPS domain consists of about 50 aa residues, including 4 cysteine residues and 1 cleavage site, in all homologous GPCRs, the GPS domain is located in the extracellular portion of the receptors immediately adjacent to the first transmembrane segment [19,20]. The GPS domain contains a putative proteolytic site that appears to be conserved in a number of homologous adhesion GPCRs; the cleavage sites for the extracellular portion of the receptors are located in the C-terminal amino acid residues of the GPS, although this region is poorly conserved among GPCRs [21]. In mBAI1, the putative proteolytic site is located in the extracellular portion before the first transmembrane region (CXCXXLST, aa 921–928). Recently, we found that BAI1's extracellular region is cleaved at three sites, and one of the cleaved fragments (BAI1-TSR) is the core extracellular fragment for BAI1's anti-proliferative activity, which is derived from the functional blocking of $\alpha_v\beta_5$ integrin in ECs [22]. Because mBAI3 also contains a GPS domain like mBAI1, the extracellular portion of mBAI3 may also be cleaved at the TSR-containing regions or GPS domain.

3.2. Brain-specific expression pattern of mBAI3

A Northern blot tissue survey was performed using an mBAI3 cDNA probe (nucleotides 3661–4056) to ascertain the developmental pattern of *mBAI3* expression. A ~6.0-kb transcript was observed only in brain of embryonic day 18 mouse tissues (Fig. 3A, upper panel). Most adult (3 months old) tissues expressed little or none of the 6.0-kb transcript, although a very high level was detected in the brain (Fig. 3B, upper panel). These results indicate that mRNAs encoding mBAI3 are the most abundant in brain regardless of developmental stages and are not expressed in other tissues. It is of interest to note that mBAI3 genes showed a more brain-specific expression pattern than mBAI2 and mBAI1, because mBAI3 has not expressed in other tissues even in the embryonic period.

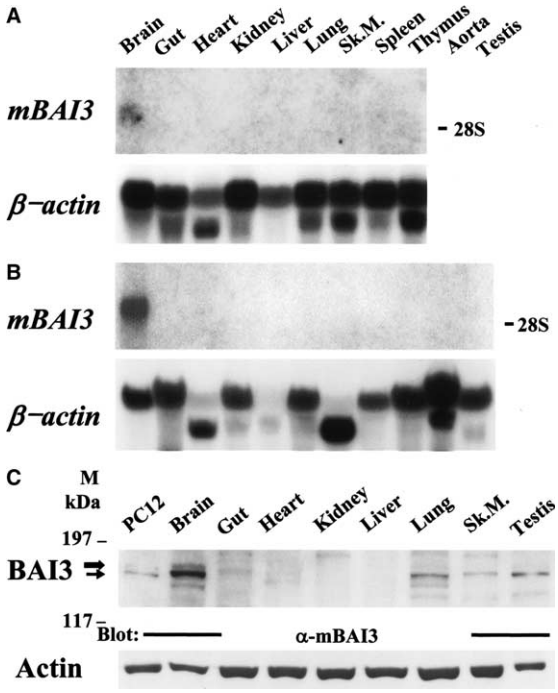

Fig. 3. Northern and Western blot analyses of mBAI3 expression in various mouse tissues. Total RNA isolated from various tissues of 18-day embryonic (A) and 3-month-old adult (B) mice was hybridized with an *mBAI3* cDNA probe. For each blot, RNA fidelity was confirmed by rehybridization with a β-actin probe (lower panels). Note that the 6.0-kb transcript was only expressed in brain of both embryonic (A) and adult (B) tissues. (C) Total tissue protein was isolated from various tissues of adult mice and reacted with polyclonal antibody against mBAI3. An upper thick arrow indicates the ~177-kDa mBAI3 protein, which shows a brain-specific expression pattern. PC12 cell, treated with neuronal growth factor (150 ng/ml) for 5 days to differentiate into neuronal cells and have the neuronal characteristics, was added as a positive control for the neuronal expression of BAI3. There was other lower band (~172 kDa band, lower thin arrow) in the brain, lung, skeletal muscle and testis recognized by a polyclonal anti-mBAI1 antibody. The molecular mass marker is shown on the left. The same blot was reprobed with anti-actin antibody to control for loading (lower panel).

To monitor the brain-specific expression pattern of mBAI3, Western blot analysis of tissue distribution was performed using a polyclonal anti-mBAI3 antibody raised against amino acids 1221–1352 of mBAI3 fused to GST. This region is localized in the unique cytoplasmic portion of mBAI3. Only the brain expressed the BAI3 protein, which appeared as a ~177 kDa band (Fig. 3C, upper thick arrow). However, there were other lower bands (~172 and ~162 kDa band) in the brain, lung, skeletal muscle and testis recognized by a polyclonal anti-mBAI3 antibody. Especially, prominent band (~172 kDa, Fig. 3C, lower thin arrow) may result from alternatively spliced variant of mBAI3, which was devoid of third loop of STR. However, this spliced transcript was not observed in the Northern blot assays because the differences of molecular size between the wild-type BAI3 and variants were relatively small, and the Northern message of mBAI3 was a little thick.

3.3. The developmental expression pattern of mBAI3 in the brain

To further characterize the developmental expression pattern of mBAI3 in the brain, RNAs were prepared from brains

of mice at embryonic day 18, early neonatal period (days 1 and 3 after birth), before and after eyelid opening (neonatal days 10, 15, 22, 29), 8 weeks, and 3 months old. The expression level of *mBAI3* increased after birth and reached its highest level during the early neonatal period. After 10 days, it decreased continuously until adult life (Fig. 4A and F). However, unlike to that of *mBAI3*, the expression of *mBAI2* or *mBAI1* reached its highest level after 10 days, but it decreased slightly after 15 days, and this level was maintained in the adult (Fig. 4B, C and F).

We performed RT-PCR analyses using specific primers flanking the TSRs and STR to investigate whether mBAI3, like mBAI2, has any alternatively spliced variants and to examine the developmental expression of any spliced variants in mouse brain. Unlike mBAI2, mBAI3 had no alternatively spliced variants of the first TSR- and/or second TSR during brain development of brain (Fig. 4G). However, RT-PCR analyses of adult brain RNA using primers flanking the third cytoplasmic loop of the STR produced 314- and 214-bp amplification products corresponding to the wild-type and a deleted sequence lacking the third loop, respectively. The identities of these RT-PCR products were confirmed by sequence analysis.

In agreement with the Northern blot results, RT-PCR analyses showed that the expression of mBAI3 was a little higher in the neonatal period than in the embryo or adult during the development of brain. However, the expression of the spliced variants lacking the third cytoplasmic loop was higher in embryonic brain than in neonatal or adult brain. These results indicate that alternative splicing produces a variant of mBAI3 lacking the third loop of the STR, but developmental expression of this variant in the brain is different from that of the spliced variants of mBAI2, which showed the same expression level from embryonic to adult brain [6]. The third cytoplasmic loop is important for the interaction of G protein in the serpentine receptors coupled to G proteins, which have STR [23]. Thus, the spliced variant of mBAI3, which did not have this third loop, may not perform certain essential functions of wild-type mBAI3. We are currently using yeast two-hybrid assay to search for G-proteins or other proteins that interact with this cytoplasmic loop. When considering that mBAI3 has several cell-binding motifs and mBAI3 is expressed at its highest level during the early neonatal period, but decreases continuously until adult life, we speculate that mBAI1 acts as an early antiangiogenic factor in the development of brain among the three BAIs.

3.4. Localization of BAI3 mRNA in the brain and developmental expression of BAI3 in the cerebral cortex

To determine the expression pattern of BAI3 in the rat brain, in situ hybridization analysis was performed with an antisense riboprobe spanning nucleotides 3661 through 4056, which is a BAI3-specific region. *BAI3* was expressed throughout most neurons of the whole cerebral cortex, but a high level was present in layers II–III and IV just as it is for *BAI1* or *BAI2* (Fig. 5A and B). It was also present in high levels in the pyramidal neurons of all fields of the hippocampus, and the granule cell and polymorphic layers of the dentate gyrus (Fig. 5A and C). In the cerebellum, the *BAI3* signal was most abundant in the Purkinje cell layer, but diffuse and very weak signals were observed in the granular and molecular layers, respectively (Fig. 5D). *BAI3* was also expressed in several nuclei of the brain stem (Fig. 5A). It was highly expressed in the hypoglossal (Fig. 5E), trigeminal motor and sensory (Fig. 5F), cochlear (Fig. 5G). It was also expressed in the pontine reticular nucleus and reticular part of substantia nigra (Fig. 5A). These observations indicate that, like BAI1

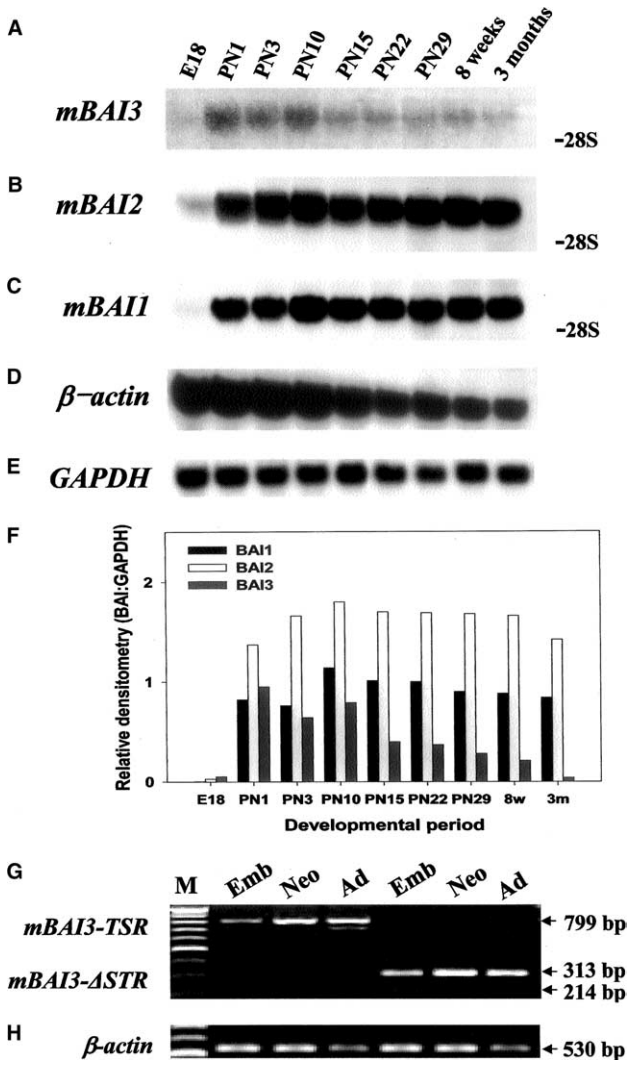

Fig. 4. Developmental expression pattern of *mBAI3* in the brain. Total mouse brain RNA from various stages of development was hybridized with a cDNA probe for *mBAI3* (A), *mBAI2* (B) or *mBAI1* (C). For each RNA blot, RNA fidelity was confirmed by rehybridization with a β-actin (D) and GAPDH (E) probes. (F) Densitometric analyses of Northern blot for BAI1, BAI2 and BAI3. Each BAI level was normalized with respect to the corresponding GAPDH level. The expression level of *mBAI3* reached its highest level at 1 day after birth (PN1). However, the expression of *mBAI3* decreased continuously after the early neonatal period through adulthood. In contrast, the expression levels of *mBAI2* and *mBAI1* increased after birth and reached their highest levels at 10 days (PN10). E18, embryonic day 18; PN1, PN3, PN10, PN15, PN22, PN29; neonatal days 1, 3, 10, 15, 22, 29 after birth. (G) RT-PCR analyses of developmental expression of alternatively spliced variants of mBAI3 in the brain. The wild-type mBAI3 with TSR and STR showed the highest level during the neonatal period. mBAI3 did not have any TSR deletion, but did have an STR-deleted sequence (mBAI3-ΔSTK). The 313-bp product corresponds to the wild-type sequence of mBAI3, and the 214-bp band corresponds to the product (mBAI3-ΔSTR) lacking the third loop of STR. Emb, embryonic day 18; Neo, neonatal day 1; Ad, 3 months old. (D, H) High levels of β-*actin* in the embryonic and early neonatal brains reflect the high cellular activities in these periods.

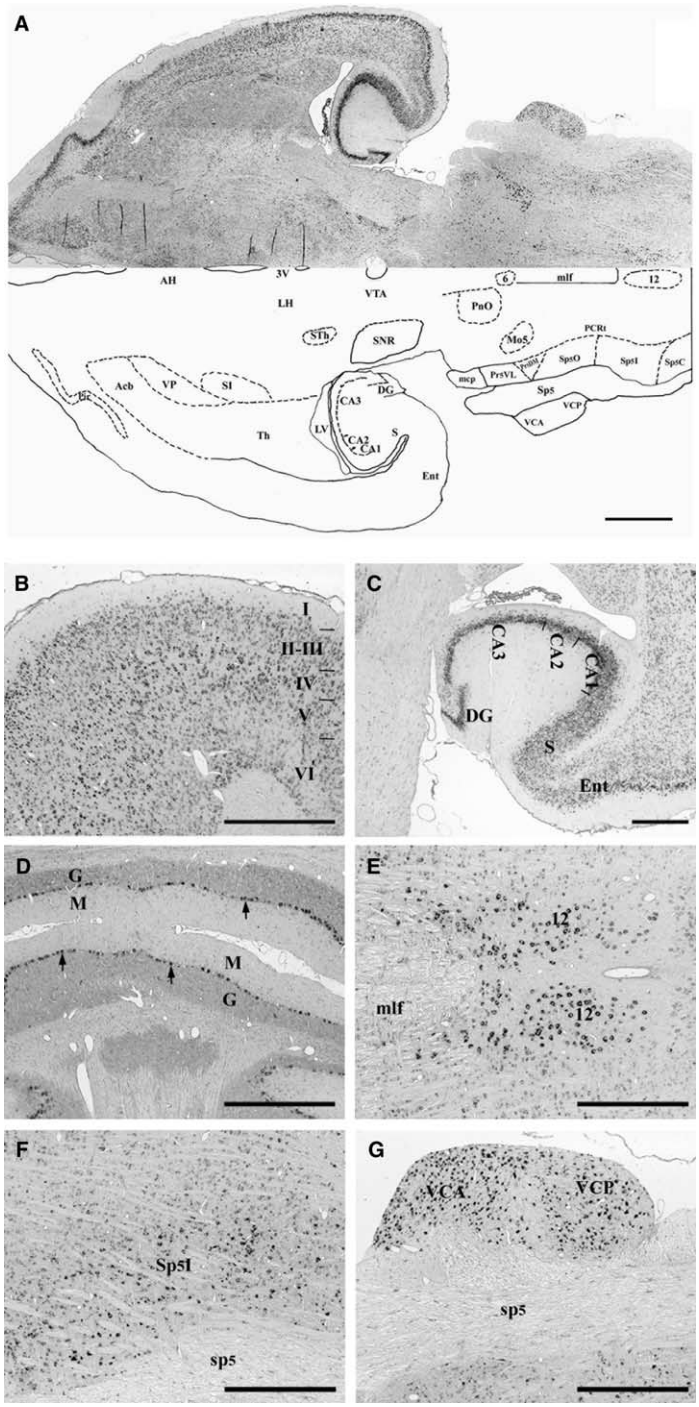

Fig. 5. In situ hybridization localization of BAI3 mRNA in several regions of adult rat brain and in several nuclei of brain stem. (A) Localization of BAI3 mRNA (upper) in the adult rat brain. Digoxigenin-labeled antisense *BAI3* probe was hybridized under stringent conditions to a horizontal section of brain (upper panel). Camera lucida drawing showing the labeled structures in the rat brain (lower panel). 3V, third ventricle; 6, abducens nucleus; 12, hypoglossal nucleus; Acb, accumbens nucleus; AH, anterior hypothalamic area; CA1, CA2, CA3; CA1, CA2, CA3 field of Ammon's horn; DG, dentate gyrus; Ent, entorhinal cortex; LH, lateral hypothalamie area; LV, lateral ventricle; mcp, middle cerebellar peduncle; mlf, medial longitudinal fasciculus; Mo5, motor trigeminal nucleus; PCRt, parvocellular reticular nucleus; Pir, piriform cortex; PnO, oral pontine reticular nucleus; Pr5DM, dorsomedial principal sensory trigeminal nucleus; Pr5VL, ventrolateral principal sensory trigeminal nucleus; S, subiculum; SI, substantia innominata; SNR, substantia nigra reticular part; sp5, spinal trigeminal tract; Sp5C, caudal spinal trigeminal nucleus; Sp5I, interpolar spinal trigeminal nucleus; Sp5O, oral spinal trigeminal nucleus; STh, subthalamic nucleus; Th, thalamic nucleus; VCA, anterior ventral cochlear nucleus; VCP, posterior ventral cochlear nucleus; Vp, ventral pallidum; VTA ventral segmental area. (B) Perirhinal cortex showed strong hybridization signals in most neurons of layers II through VI. (C) Pyramidal neurons of all fields (CA1, CA2, CA3) of Ammon's horn, and the granule cell and polymorphic layers of dentate gyrus (DG) showed high hybridization signals. (D) Cerebellar cortical sections showing strong signals in the Purkinje cells, but diffuse weak signals in the granular layers (G) and very weak signals in the molecular layers (M). (E) Strong hybridization signals were found in the large neurons of the hypoglossal nucleus. (F) Signals were detected in the interpolar spinal trigeminal nucleus. (G) Very strong signals were detected in the anterior and posterior ventral cochlear nucleus. Scale bars (A), 500 μm; (B–G), 200 μm.

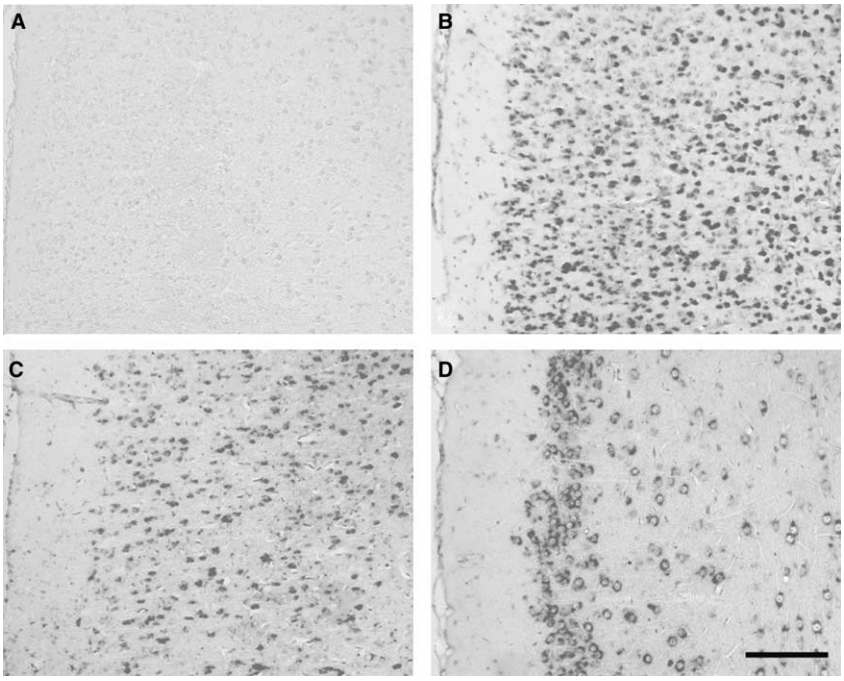

Fig. 6. Developmental expression *of BAI3* in cerebral cortex. Cerebral cortex of the rat brain was hybridized digoxigenin-labeled sense (A, 2 weeks, negative control) and antisense *BAI3* probe (B, C, D) at time points after birth (2, 3 and 8 weeks). (B) At 2 weeks, a high activity of the *BAI3* was detected throughout the whole cerebral cortex. (C) At 3 weeks, the expression level of the *BAI3* decreased slightly in the whole cerebral cortex. (D) At 8 weeks, the expression level of the *BAI3* decreased generally in the whole cerebral cortex, but it showed a relative strong hybridization signal in most neurons of layers II–III. Scale bar, 50 μm.

and BAI2, BAI3 is a neuron-specific protein, and that the localization of BAI3 expression in the brain coincides with that of BAI1 or BAI2.

To confirm the Northern data that the neonatal brain has higher levels of *BAI3* expression than the adult, in situ hybridization experiment was performed to the neonatal cerebral cortex of 2, 3 and 8 weeks-old brain (Fig. 6). At 2 weeks, a high activity of the *BAI3* was detected throughout the whole cerebral cortex (Fig. 6B). *BAI3* decreased slightly in the whole cerebral cortex at 3 weeks (Fig. 6C), but decreased generally at 8 weeks (Fig. 6D). However, it showed a strong hybridization signal in most neurons of layers II–III at 8 weeks. These results indicate that BAI3 was highly expressed in neonatal brain, and it was derived from neuron-specific expression, but not from the result of glial expression of BAI3.

3.5. Changes in *BAI3* expression in focal ischemia

To investigate the role of BAI3 in ischemia-induced brain angiogenesis, the temporal expression profiles of BAI3 and VEGF in ischemic cerebral tissues were measured in the in vivo focal cerebral ischemia model. Western blot analyses of the ischemic portion of the cerebral cortex using specific antibodies recognized ~170- and ~25-kDa bands corresponding to BAI3 and VEGF proteins, respectively. The expression of BAI3 decreased on the ischemic side of the brain at 0.5 h after ischemia until 8 h, compared with sham-operated cerebral cortex, but it slowly recovered by 24 h (Fig. 7A). BAI3 level was significantly decreased throughout all experimental periods compared with that of control (Fig. 7D). The level of VEGF expression was transiently increased in the ischemic cortex at 0.5 h, peaked at 8 h, and it returned to basal level at 24 h after ischemia (Fig. 7B). VEGF level was significantly increased at 8 h compared with that of control (Fig. 7D).

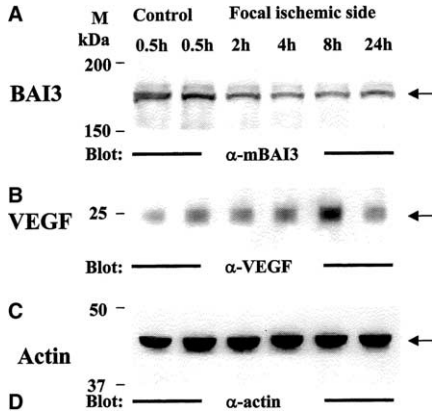

Fig. 7. Western blot analysis of BAI3 in ischemic cerebral tissues. (A) Expression of BAI3 (arrow) decreased in the ischemic side at 0.5 h after ischemia until 8 h compared with sham-operated cerebral cortex (Control), but returned slowly to its basal level after 24 h. (B) VEGF increased at 0.5 h, peaked at 8 h, and returned to its basal level at 24 h. (C) The same blot was reprobed with anti-actin antibody to control for loading. The molecular mass marker is shown on the left. (D) Densitomeric analyses of Western blot for BAI3 and VEGF. BAI3 or VEGF level was normalized with respect to the corresponding actin level. The reported values are the means ± S.E.M. of 3 observations. Significance of difference of relative BAI3 or VEGF level (ratio of BAI3 or VEGF versus actin densitometric value) in each period compared with control one was tested by Student's *t*-test (**$P < 0.01$, ***$P < 0.001$).

The ischemic brain might stimulate angiogenesis to compensate for impaired circulation. TSP1 and TSP2 are naturally occurring angiostatic factors that inhibit angiogenesis in vivo and in vitro. The roles of TSP and BAIs in the regulation of postischemic angiogenesis are not completely known. Re-

cently, we reported that angiostatic BAI2 participated in ischemia-induced brain angiogenesis in concert with angiogenic VEGF. The expression of *BAI2* decreased in the ischemic side of cerebral cortex after 1 h compared with sham-operated one and the decreased level was maintained at 2 h, but was slowly recovered after 8 h. Whereas, *VEGF* reached its peak level in the ischemic cerebral cortex and contralateral non-ischemic one after 8 h, but was returned to control level at 24 h [6]. Thus, BAI3 and VEGF showed reciprocal expression patterns in in vivo focal ischemic model, just as BAI2 and VEGF do [6], but BAI3 participated in the earlier phases of ischemia-induced angiogenesis than BAI2. In the in vitro hypoxic model with cobalt chloride, BAI3 mRNA expression decreased at 0.5 h after hypoxia, but returned to the control value at 2 h and decreased again at 8 h. In contrast, TSP1 mRNA increased at 2 h, but recovered to its basal level at 24 h after ischemia (data not shown). These results indicate that BAI3 decreased earlier than BAI2 and BAI1, but the expression pattern of TSP1 was different from that of BAI3. Lin et al. [24] reported that TSP1 and TSP2 are differently regulated after focal cerebral ischemia/reperfusion. The expression of TSP1 occurred early in a biphasic fashion, while TSP2 was expressed in a delayed monophasic manner. Collectively, among the three BAIs, BAI3 seemed to act in the earlier phases of ischemia-induced brain angiogenesis as well as an earlier antiangiogenic factor in the development of the brain.

3.6. Changes in angiostatic and angiogenic genes in human gliomas

We also examined the expression of angiostatic and angiogenic genes in different grades of tumors to study the relationship between BAIs and the progression of human gliomas. We performed RT-PCR analyses of 17 human brain specimens. The expression of BAI1 mRNA was observed in most human gliomas except three cases of ependymomas (#4 and #5 ependymomas, #9 anaplastic ependymoma) (Fig. 8A). The expression of BAI2 mRNA was lower in all grade III samples compared to normal brain tissue, though the difference was small (Fig. 8B). Also, the expression of *BAI3* was lower in grade III gliomas and IV glioblastoma compared with normal brain (Fig. 8C). In particular, *BAI3* was barely expressed in ependymoma (#4) among low-grade and anaplastic ependymoma (#9) among grade III. Thus, our results indicated that the expressions of BAI1, BAI2, and BAI3 mRNAs in low-grade human gliomas were not changed compared with the normal brain except for ependymomas (#4 and #5), and the expression of *BAI3* was generally lower in high-grade gliomas. In contrast, normal brain and low-grade glioma did not express *VEGF* and *HIF-1*α except the ependymomas (#4 and #5). However, *VEGF* expression was almost exclusively observed in the grade III and IV tumors (Fig. 8D). In the majority of these high-grade tumors, upregulation of HIF-1α mRNA above that of low-grade tumors, was also observed (Fig. 8E). *TSP1, a* well-known angiostatic factor, was highly expressed in high-grade tumors (Fig. 8F), indicating that the regulation of TSPI was different from that of BAIs in malignant gliomas. Also, *p53* was expressed more in high-grade than in low-grade gliomas, especially in anaplastic oligodendrogliomas (#11 and #12) (Fig. 8G).

Glioblastoma represents 15–20% of brain tumors and 50% of all gliomas [25]. VEGF is a hypoxia-inducible angiogenic factor that is known to be upregulated in most cases of glio-

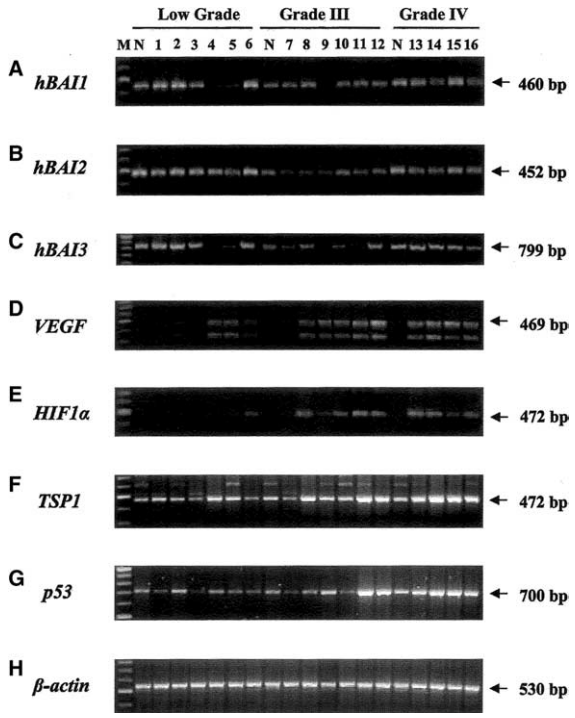

Fig. 8. RT-PCR analyses of angiostatic (BAI1, BAI2, BAI1, TSPl) and angiogenic (VEGF and HIF-1α) genes in human gliomas. Expression was examined in various grades of gliomas by RT-PCR analyses of 17 human brain samples. (A) The expression of *BAI1* was observed in most human gliomas except 3 cases of ependymomas (#4 and #5 ependymomaa and #9 anaplastic ependymoma). (B) The expression of *BAI2* was reduced in all grade III samples compared to normal brain tissue, though the difference was small. (C) The expression of *BAI3* decreased in grade III and IV gliomas. In particular, *BAI3* was barely detectable in ependymoma (#4) and anaplastic ependymoma (#9). Normal brain and low-grade glioma did not express *VEGF* (D) or *HIF-1*α (E) except ependymomas (#4 and #5), and *VEGF* expression was almost exclusively observed in the grade III and IV tumors (D). (E) HIF-1α mRNA was also upregulated in high-grade tumors compared to low-grade tumors. (F) *TSP1* was highly expressed in high-grade gliomas. (G) *p53* was expressed more in high-grade than low-grade gliomas and especially in anaplastic oligodendrogliomas (#11 and #12). (H) The result β-*actin* (530 bp) confirmed the relative amount and fidelity of the total RNA samples. N, Normal brain tissue.

blastomas. Kaur et al. [9] reported that BAI1 was widely expressed in normal brain but was absent in 28 glioma cell lines and in the majority of human glioblastomas. In this study, we examined whether the expressions of anti-angiogenic BAIs differed in different grades of human gliomas. Expression of BAI3 was generally decreased in malignant gliomas, whereas angiogenic genes, such as VEGF and HIF-1α were increased. In the real-time RT-PCR analyses, the relative expression levels of BAI1 in normal brain tissue and SHSY5Y neuroblastoma cells were highest among BAIs, and the generally decreased expressions of BAIs in high-grade glioma compared to normal tissue (higher cycle-threshold values in high-grade glioma than normal brain) were observed (data not shown) [26]. Thus, the expression levels of three BAI genes in the brain tumor tissues could be used for the prediction of malignancy. However, TSP1 was expressed more in most human gliomas than normal brain and showed a different expression pattern compared to BAIs. Sasaki et al. [27] reported that TSP1 secreted by malignant glioma cell lines participates in the

activation of latent TGF-β in malignant glioma cells. Although it acts as an inhibitor of tumor growth, TSP1 is sometimes expressed at high levels during tumor progression, suggesting that tumors can eventually overcome its anti-tumor effects [28]. Thus, our results indicate that brain-specific angiostatic BAIs also may participate in the regulation of malignant progression of gliomas, and suggest that BAIs may have more suppressive effects on brain tumor progression than TSP1.

The p53 tumor suppressor gene is frequently mutated in human cancer, and is important in the pathogenesis of central nervous system tumors [25]. Most of the mutations in the p53 gene occur in its DNA-binding domain. Every residue contained in this domain (aa 110–286), with one exception, has been found to be the target of substitutions in human cancers. The most frequently mutated residues (R175, G245, R248, R249, R273 and R282) account for about 30% of all known mutations [29,30], In this study, p53 mRNA was highly expressed in grade III (anaplastic oligodendroma) and IV (glioblastoma) tumors, whereas BAIs were generally decreased in these stages of glioma. Because BAI1 is induced by wild-type p53 in cultured glial cells and pancreatic adenocarcinoma cells [1,31], we examined whether there were reported or unknown mutations of p53 in the malignant gliomas in which BAIs were decreased or not expressed. We produced RT-PCR amplification products using primers flanking the reported p53 point mutation region (exon 5–7 and part of exon 8) from normal tissue and human gliomas (ependymoma, anaplastic oligodendroma and glioblastoma), and these fragments were sequenced (data not shown). Especially, besides the well-known mutations, the sequence analysis of p53 from one ependymoma in which BAI1 and BAI3 were not expressed revealed point mutations of 2 amino acids. This pair of p53 mutations has not been previously reported: Arg72Pro (exon 5) and Tyr220Cys (exon 6).

Collectively, our results indicated that neuron-specific BAI3 participates in the earlier phase of ischemia-induced brain angiogenesis than BAI1 and BAI2, and brain-specific angiostatic BAIs were involved in the regulation of brain tumor progression. The decreased level of three BAI genes in glioma tissues could be used as one of the molecular markers for the prediction of high-grade glioma.

Acknowledgements: We thank Song Eun Lee for assisting immunohistochemistry and Jennifer Macke for editing the text. This study was financially supported by special research fund of Chonnam National University in 2004.

References

[1] Nishimori, H., Shiratsuchi, T., Urano, T., Kimura, Y., Kiyono, K., Tatsumi, K., Yoshida, S., Ono, M., Kuwano, M., Nakamura, Y. and Tokino, T. (1997) Oncogene 15, 2145–2150.
[2] Koh, J.T., Lee, Z.H., Ahn, K.Y., Kim, J.K., Bae, C.S., Kim, H.-H., Kee, H.J. and Kim, K.K. (2001) Mol. Brain Res. 87, 223–237.
[3] Tolsma, S.S., Volpert, O.V., Good, D.J., Frazier, W.A., Polverini, P.J. and Bouck, N. (1993) J. Cell. Biol. 122, 497–511.
[4] Adams, J.C. and Tucker, R.P. (2000) Dev. Dyn. 218, 280–299.
[5] Shiratsuchi, T., Nishimori, H., Ichise, H., Nakamura, Y. and Tokino, T. (1997) Cytogenet. Cell Genet. 79, 103–108.
[6] Kee, H.J., Koh, J.T., Kim, M.Y., Ahn, K.Y., Kim, J.K., Bae, C.S., Park, S.S. and Kim, K.K. (2002) J. Cereb. Blood Flow Metab. 22, 1054–1067.
[7] Piesch, T., Valter, M.M., Wolf, H.K., Deimling, A., Huang, H.J.S., Cavenee, W.K. and Wiestler, O.D. (1997) Acta Neuropathol. 93, 109–117.
[8] Harrigan, M.R. (2003) Neurosurgery 53, 639–661.
[9] Kaur, B., Brat, D.J., Calkins, C.C. and Van Meir, E.G. (2003) Am. J. Pathol. 162, 19–27.
[10] Lee, Z.H., Kim, H-H., Ahn, K.Y., Seo, K.H., Kim, J.K., Bae, C.S. and Kim, K.K. (2000) Mol. Brain Res. 75, 237–247.
[11] Volpert, O.V., Tolsma, S.S., Pellerin, S., Feige, J.J., Chen, H., Mosher, D.F. and Bouck, N. (1995) Biochem. Biophys. Res. Commun. 217, 326–332.
[12] Jimenez, B., Volpert, O.V., Crawford, S.E., Febbraio, M., Silverstein, R.L. and Bouck, N. (2000) Nat. Med. 6, 41–48.
[13] Qabar, A.N., Bullock, J., Matej, L. and Polverini, P. (2000) Biochem. J. 346, 147–153.
[14] Shafiee, A., Penn, J.S., Krutzsch, H.C., Inman, J.K., Roberts, D.D. and Blake, D.A. (2000) Invest. Ophthalmol. Vis. Sci. 41, 2378–2388.
[15] Asch, A.S., Liu, I., Briccetti, F.M., Barnwell, J.W., Kwakye-Berko, F., Dokun, A., Goldberger, J. and Pernambuco, M. (1993) Science 262, 1436–1440.
[16] Dawson, D.W., Pearce, S.F., Zhong, R., Silverstein, R.L., Frazier, W.A. and Bouck, N.P. (1997) J. Cell Biol. 138, 707–717.
[17] Fearon, D.T. and Austen, K.F. (1975) J. Exp. Med. 142, 856–863.
[18] Higgins, J.M., Wiedemann, H., Timpl, R. and Reid, K.B. (1995) J. Immunol. 155, 5777–5785.
[19] Fredriksson, R., Gloriam, D.E.I., Hoglund, P.J., Lagerstrom, M.C. and Schoith, H.B. (2003) Bioehem. Biophys. Res. Commun. 301, 725–734.
[20] Kierszenbaum, A.L. (2003) Mol. Reprod. Dev. 64, 1–3.
[21] Krasnoperov, V., Lu, Y., Buryanovsky, L., Neubert, T., Ichtchenko, K. and Petrenko, A. (2002) J. Biol. Chem. 277, 46518–46526.
[22] Koh, J.T., Kook, H., Kee, H.J., Seo, Y.W., Jeong, B.C., Lee, J.H., Kim, M.Y., Yoon, K.C., Jung, S. and Kim, K.K. (2004) Exp. Cell Res. 294, 172–184.
[23] Stefan, C.J. and Blumer, K.J. (1994) Mol. Cell. Biol. 14, 3339–3349.
[24] Lin, T.N., Kim, G.M., Chen, J.J., Cheung, W.M., He, Y.Y. and Hsu, C.Y. (2003) Stroke 34, 177–186.
[25] Yoon, K.S., Lee, M.C., Kang, S.S., Kim, J.H., Jung, S., Kim, Y.J., Lee, J.H., Ahn, K.Y., Lee, J.S. and Cheon, J.Y. (2001) J. Korean Med. Sci. 16, 481–488.
[26] Gutala, R.V. and Reddy, P.H. (2004) J. Neurosci. Methods 132, 101–107.
[27] Sasaki, A., Naganuma, H., Satoh, E., Kawataki, T., Amagasaki, K. and Nukui, H. (2001) Neurol. Med. Chir. (Tokyo) 41, 253–258.
[28] Filleur, S., Volpert, O.V., Deeorges, A., Voland, C., Reiher, F., Clézardin, P., Bouck, N. and Cabon, F. (2001) Genes Dev. 15, 1373–1382.
[29] Smith, N.D., Rubenstein, J.N., Eggener, S.E. and Kozlowski, J.M. (2003) J. Urol. 169, 1219–1228.
[30] Szymanska, K. and Hainaut, P. (2003) Acta Biochim. Pol. 50, 231–238.
[31] Duda, D.G., Sunamura, M., Lozonschi, L., Yokoyama, T., Yatsuoka, T., Motoi, F., Horii, A., Tani, K., Asano, S., Nakamura, Y. and Matsuno, S. (2002) Br. J. Cancer 86, 490–496.